ISSN 1070-3632, Russian Journal of General Chemistry, 2014, Vol. 84, No. 11, pp. 2107–2113. © Pleiades Publishing, Ltd., 2014.
Original Russian Text © S.N. Golubev, N.Sh. Lebedeva, Yu.A. Gubarev, A.I. V'yugin, V.P. Andreev, 2014, published in Zhurnal Obshchei Khimii, 2014, Vol. 84, No. 11, pp. 1809–1816.

Thermo-Oxidative Degradation of Styryl Derivatives of Pyridine-*N*-Oxides

S. N. Golubev[a], N. Sh. Lebedeva[a], Yu. A. Gubarev[a], A. I. V'yugin[a], and V. P. Andreev[b]

[a] *Krestov Institute of Solutions Chemistry of the Russian Academy of Sciences, ul. Akademicheskaya 1, Ivanovo, 153045 Russia*
e-mail: gua@isc-ras.ru

[b] *Petrozavodsk State University, Petrozavodsk, Russia*

Received September 23, 2013

Abstract—Kinetic parameters of thermo-oxidative degradation of various derivatives of pyridine-*N*-oxide have been calculated. Thermo-oxidative degradation is a multi-stage process. 4-Substituted pyridine-*N*-oxides are more thermally stable than the 2-substituted isomers. Stability of 4-substituted pyridine-*N*-oxides towards thermo-oxidation is enhanced in the presence of electron-donating ability of the substituent. In the case of 4-styrylpyridine-*N*-oxide, the rate-limiting stage of thermo-oxidation is a chemical reaction; for other studied compounds, the limiting stage is free nucleation and further nuclei growth.

Keywords: styryl, pyridine-*N*-oxide, thermo-oxidative degradation, crystal hydrate

DOI: 10.1134/S1070363214110115

Various *N*-oxides are common in biosphere; they are known for a wide range of biological activity. For example, they may act as growth regulators, mutagens, and carcinogens. In particular, the increased incidence of gastroenteric oncological diseases in coastal countries has been attributed to high content of amines in the thermally treated seafood products, efficiently accumulating trimethylamine *N*-oxide [1]. *N*-Oxide are often recognized as metabolites of biologically active compounds, for example, of neuroleptic Clozapine [2] and of alkaloid nicotine [3]. At the same time, reports on degradation routes of *N*-oxides are practically absent in the literature.

N-Oxides are known for diverse chemical properties; hence, they are widely applied in various branches of science and technology. For example, *N*-oxides of quaternary amines are very special organic compounds capable of efficient solvents for cellulose [4, 5]. Significant drawback of *N*-oxides limiting their application in cellulose industry is the low thermal stability. According to [5], the N→O bond strength in *N*-oxides of heterocyclic unsaturated amines is of about 220 kJ/mol. Heat of degradation of *N*-methylmorpholine-*N*-oxide (the best solvent for cellulose) is of 159 kJ/mol. It has been stated [5–7] that *N*-oxides thermo-oxidation reactions follow the general mechanism involving elimination of oxygen and formation of the corresponding heterocyclic amine. On the contrary, other studies [8–10] have revealed already the first stage of *N*-oxides thermo-oxidative degradation results in a complex mixture of products; in particular, the intramolecular transfer of oxygen from N→O can occur, resulting in phenols and their derivatives [9] or ethers [8, 10]. Evidently, detailed studies of thermo-oxidative degradation of *N*-oxides are of considerable interest for various fields of industry and medicine. Study of thermo-oxidative degradation is complicated by the simultaneous intense heat evolution that in turn affects the reaction rate. Due to the high pressure, the reaction products are formed in the condensed state and can therefore participate in the secondary reactions [11]. Mechanism of thermo-oxidative degradation can be changed with temperature [12], further complicating the results interpretation. On top of that, the results obtained using differential scanning or adiabatic calorimeter can be disfigured due to the secondary reactions involving gaseous products formed in the closed volume. Thermogravimetric analysis seems far more convenient; this approach was

Scheme 1.

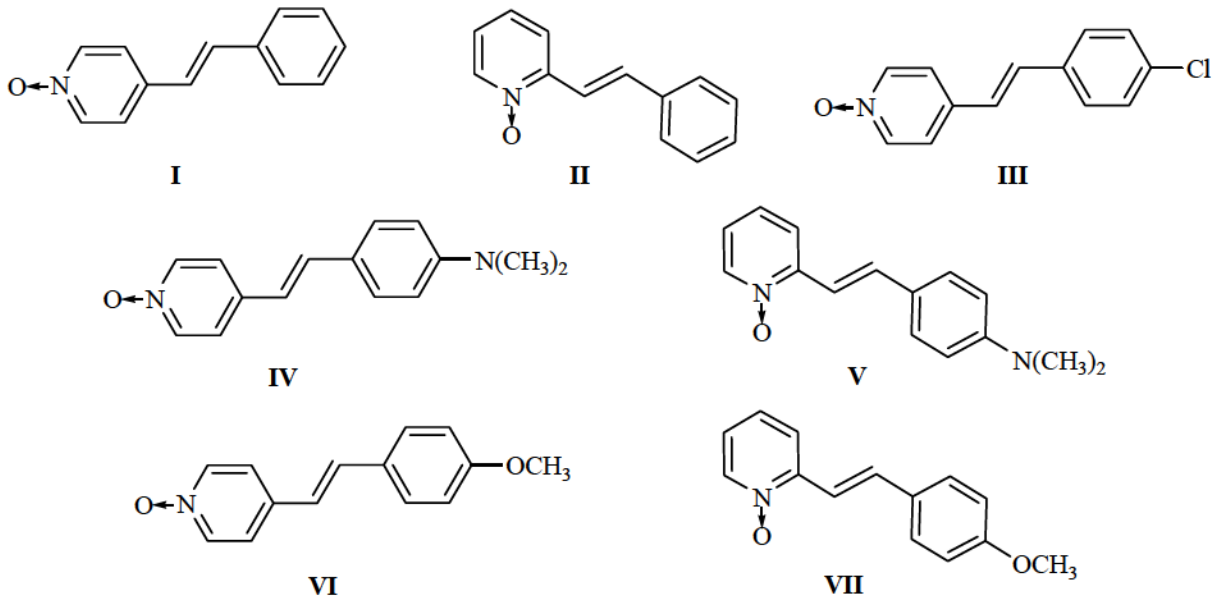

used throughout this work to investigate kinetics of thermo-oxidative degradation of heterocyclic *N*-oxides, extending the previously reported studies [13]. Structural formula of the studied compounds are given in Scheme 1.

Figures 1–4 show typical thermograms of thermo-oxidative degradation of selected *N*-oxides.

Thermo-oxidative degradation of heterocyclic *N*-oxides occurred in several stages, as evidenced by complex shape of the curves in Figs. 1–4 and results of their processing (Table 1).

In the cases of some *N*-oxides, slight weight loss was observed at temperature below 450 K (stage 1: Table 1, Figs. 1a–4a). At the same time, the electronic absorption spectra of the studied compounds were not changed; likely, loss of mass at stage 1 was due to elimination of water (either contained in crystal hydrate or occluded during crystallization) rather than due to thermo-oxidative reactions. Physico-chemical parameters of crystal hydrates of the studied *N*-oxides determined following the procedure described in [14] are collected in Table 2.

Noteworthily, the measured enthalpies of water evaporation from crystal hydrates were determined with significant error because the quasi-equilibrium condition was not held at the selected heating rate. Nevertheless, the obtained data allowed estimation of *N*-oxides affinity towards specific interaction with water molecules.

For all *N*-oxides forming crystal hydrates (except for 4-styrylpyridine-*N*-oxide **I**) enthalpy of water evaporation from the hydrate exceeded that of pure water (44.5 kJ/mol [15]) confirming specific interaction of the *N*-oxides with water. In the case of compound **I**, the $\Delta_v H$ value and the non-typical composition of the crystal hydrate (**I**·1/2H_2O) suggested that water molecules were occluded into the voids of crystal lattice of the *N*-oxide.

The insufficient accuracy of $\Delta_v H$ determination did not allow quantitative determination of the substituents influence on the *N*-oxides interaction with water. Likely, the affinity of *N*-oxides to water decreased in the **VI** > **III** > **I** > **IV** series. That series did not coincide with the change of the Hammett σ-constants of peripheral substituents of the *N*-oxides (Table 2). Probably, the affinity towards water was affected by electronic effects of the substituents as well as by the crystal lattice density and the mesomeric effect of the substituents; the latter effect was enhanced with the increased conjugation system length demonstrating the absence of specific solvation of 2-substituted *N*-oxides with water.

Noteworthily, melting point of the *N*-oxide **II** (308 K) was noticeably low than that of the other studied *N*-oxides.

The second stage of thermo-oxidative degradation of the studied *N*-oxides (Table 1) was assigned to chemical transformations as evidenced by noticeable

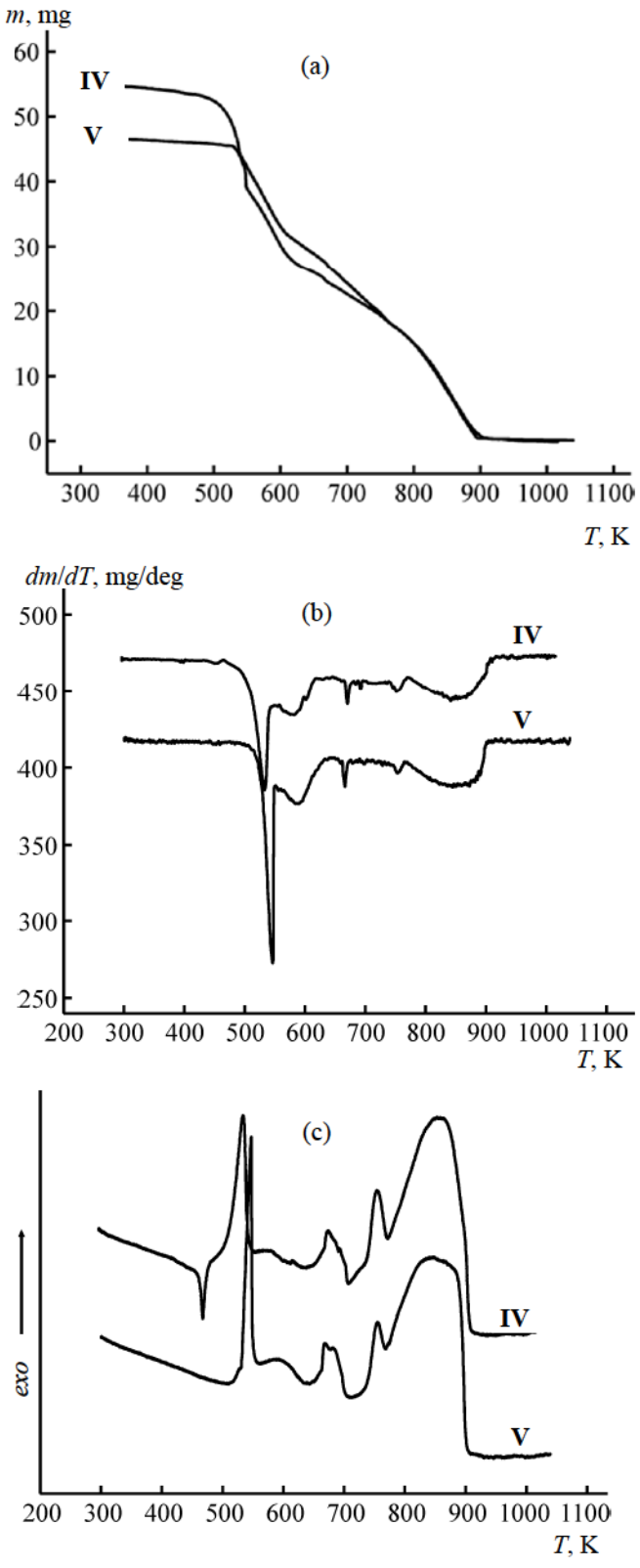

Fig. 1. Evolution of mass (a), mass change rate (b), and data of differential thermal analysis (c) in the course of thermo-oxidative degradation of *N*-oxides **IV** and **V**.

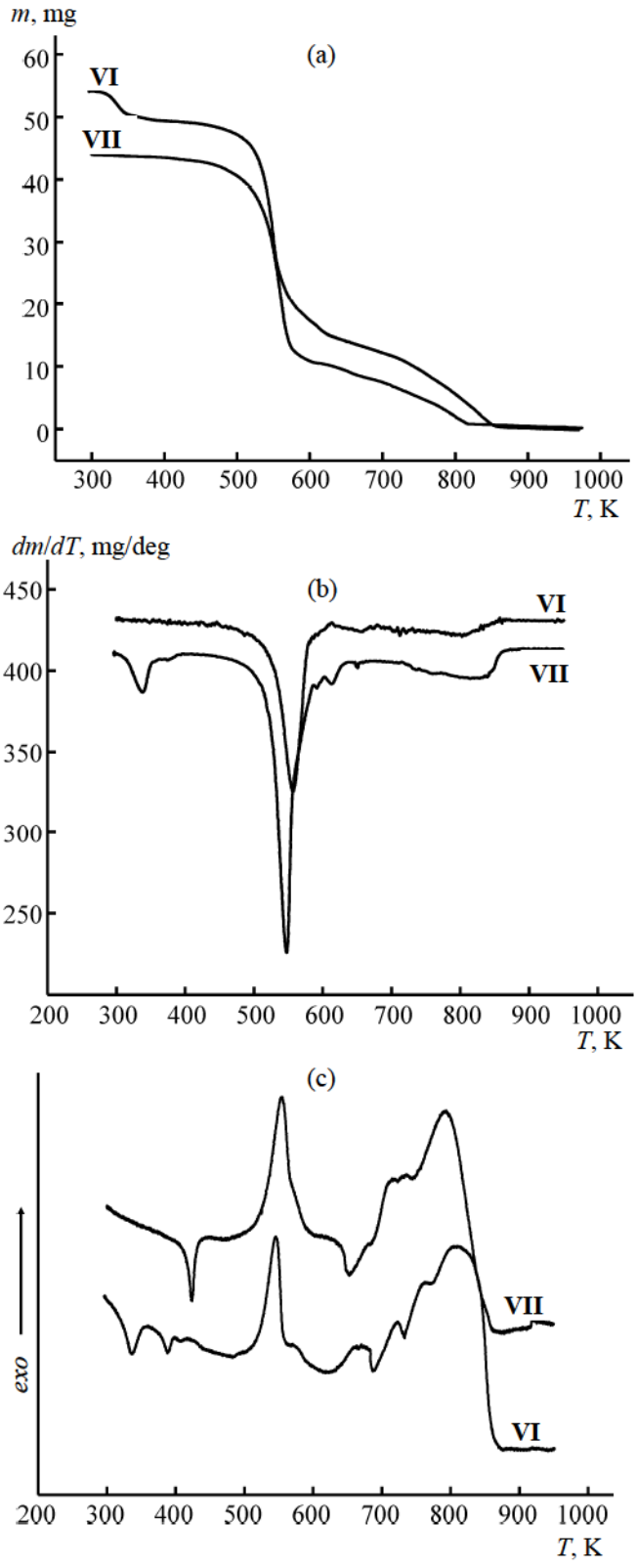

Fig. 2. Evolution of mass (a), mass change rate (b), and data of differential thermal analysis (c) in the course of thermo-oxidative degradation of *N*-oxides **VI** and **VII**.

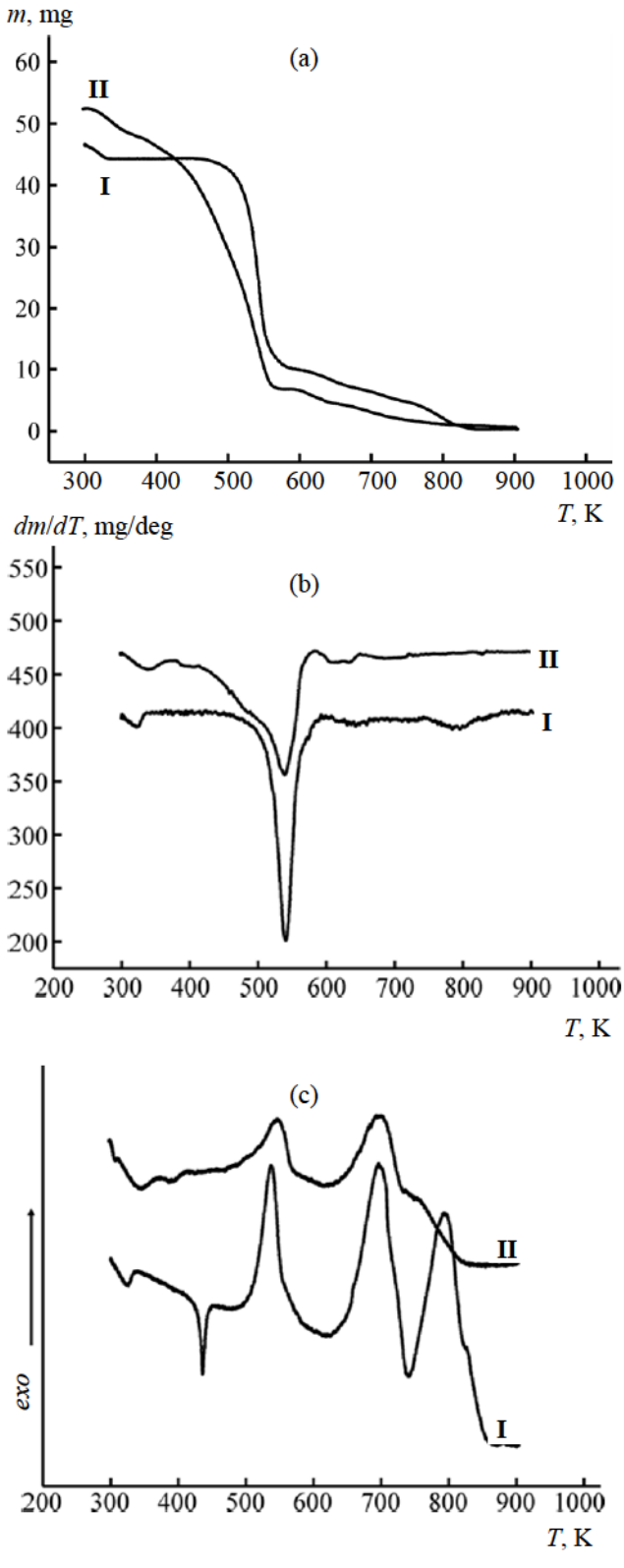

Fig. 3. Evolution of mass (a), mass change rate (b), and data of differential thermal analysis (c) in the course of thermo-oxidative degradation of *N*-oxides **I** and **II**.

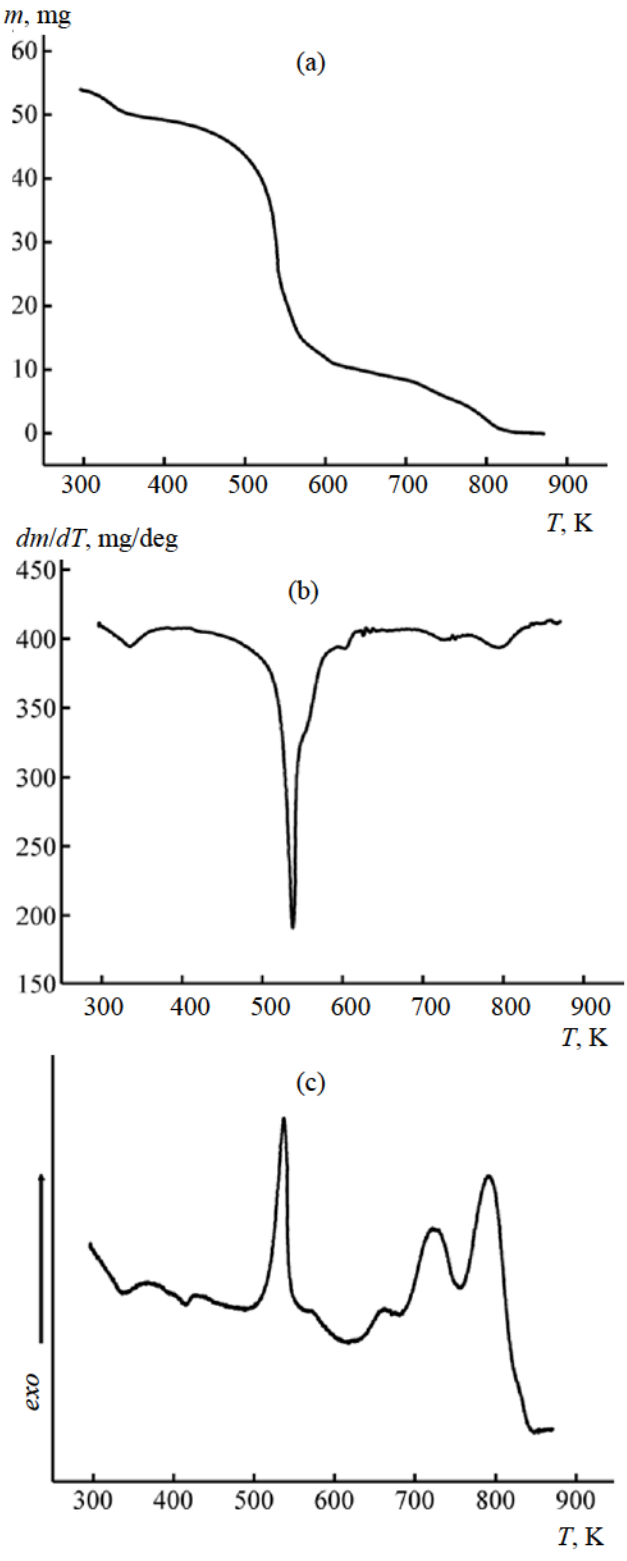

Fig. 4. Evolution of mass (a), mass change rate (b), and data of differential thermal analysis (c) in the course of thermo-oxidative degradation of *N*-oxide **VII**.

Table 1. Temperature ranges (K) of the stages of thermo-oxidative degradation

N-Oxide	Stage 1	Stage 2	Stage 3	Stage 4	Stage 5
I	<345	494–603	634–745	745–871	–
II	<370	491–622	622–729	729–856	–
III	<373	491–549	549–619	619–686	686–859
IV	–[a]	500–553	553–643	643–718	718–925
V	–	468–553	553–639	639–715	757–862
VI	<373	481–562	562–617	617–690	690-886
VII	–	493–566	566–619	620–686	686–873

[a] ("–") is the stage was not observed in the experiment.

Table 2. Physico-chemical parameters of crystal hydrates and the Hammett constants of the substituents in pyridine ring of the *N*-oxides

N-Oxide	Molar ratio of the *N*-oxide and water	T_d, K [a]	$\Delta_v H$, kJ/mol[b]	T_m, K [c]	σ_{PyO} [24]
I	2 : 1	304	32	468	–0.16
II	1 : 1	301	58	308	–
III	1 : 1	302	45	417	–0.11
IV	–[d]	–	–	–[e]	–0.4
V	–[d]	–	–	468	–
VI	1 : 1	316	60	391	–0.26
VII	–[d]	–	–	426	–

[a] Temperature of the hydrate decomposition. [b] Heat of vaporization of hydrate water. [c] Melting point of the *N*-oxide. [d] Does not form crystal hydrate. [e] Could not be determined due to overlap with other peaks.

exothermic effect (Figs. 1c–4c) and the associated changes of electronic absorption spectra upon heating.

The thermograms reflecting thermo-oxidative degradation of compounds **IV** and **V** were practically identical (Fig. 2), suggesting the similar mechanism of 2- and 4-substituted *N*-oxides degradation.

Stability of the 4-substituted *N*-oxides towards thermo-oxidative degradation as estimated from activation energy of stage 2 (Table 3) decreased in the following series (1): **IV** > **VI** > **I** > **II**.

The above-shown series correlated with the Hammett σ-constants determined for the substituted benzoic acids [16] and with σ_{PyO} constants of pyridine-*N*-oxide derivatives (Table 2). It could be suggested that the electron-donating substituents increased the electron density at the bridging moiety –CH=CH– thus strengthening the N→O bond of the *N*-oxide. Noteworthily, the weight loss of the samples at stage 2 (Table 4) did not coincide with oxygen fraction in the *N*-oxides. Hence, the suggestion that thermal degradation of *N*-oxides starts with oxygen elimination [5–7] was not always true.

Weight loss of the studied *N*-oxides at stage 2 was of 17 to 90% (Table 3). Evidently, the composition of thermo-oxidation products was affected by the nature of peripheral substituents. Interestingly, thermograms of degradation of isomeric *N*-oxides (**V** and **VI**) (Fig. 1) and (**VI** and **VII**) (Fig. 2) were almost identical, pointing at the same condensed-phase products formed at stage 2. At the same time, the high-temperature stages of degradation were significantly different in the case of isomers (**I** and **II**) (Fig. 3).

2-Substituted pyridine-*N*-oxides were less thermally stable that the corresponding 4-substituted isomers. Thermal stability of 2-substituted *N*-oxides decreased in the series (2): **II** > **V** > **VII**.

Table 3. Kinetic parameters of stage 2 of thermo-oxidative degradation of the *N*-oxides

N-Oxide	E_a, kJ/mol	ln A[a]	$f(\alpha)$	r^2
I	245	54	$4(1-\alpha)^{3/4}$	0.990
II	279	63	$2(1-\alpha)[-\ln(1-\alpha)]^{1/2}$	0.997
III	223	47	$4(1-\alpha)[-\ln(1-\alpha)]^{3/4}$	0.997
IV	325	72	$2(1-\alpha)[-\ln(1-\alpha)]^{1/2}$	0.998
V	215	47	$2(1-\alpha)[-\ln(1-\alpha)]^{1/2}$	0.997
VI	297	61	$2(1-\alpha)[-\ln(1-\alpha)]^{1/2}$	0.996
VII	155	26	$2(1-\alpha)[-\ln(1-\alpha)]^{1/2}$	0.991

[a] Pre-exponential factor in the Arrhenius equation.

Table 4. Weight loss (%) in the course of thermo-oxidative degradation of the studied *N*-oxides[a]

N-Oxide	Stage 1	Stage 2	Stage 3	Stage 4	Stage 5
I	4.3	77	81	100	[b]
II	8.7	90	96	100	[b]
III	8.8	63.8	86.9	91.2	100
IV	0	17	41	51	100
V	0	27	50	64	100
VI	8.6	57.2	74.6	82	100
VII	0	57.2	70.3	75.6	100

[a] The total weight loss at the given stage and at the previous stages. [b] Degradation was complete at stage 4.

Discrepancy of the series (1) and (2) was due to mesomeric effect of the substituents having an impact on the heterocycle stability towards thermo-oxidation.

For all the studies *N*-oxides except for compounds **I** and **III**, kinetics of thermo-oxidative degradation was followed the $d\alpha/dt = kf(\alpha)$ with $f(\alpha) = 2(1-\alpha)[-\ln(1-\alpha)]^{1/2}$ equation. Hence, the rate-limiting stages of thr overall thermo-oxidation process were free nucleation and the nuclei growth, the formal reaction rate order being of $n = 2$ [17]. In the case of *N*-oxide **III**, the limiting stage was the same, but the reaction rate order was of $n = 4$ (Table 3). In other words, the thermal degradation started with formation of the reactive sites. Their appearance distorted the compound crystal lattice, favoring formation of further reactive sites. Rate of the topochemical reaction exponentially increased with temperature until merging of the reaction product zone around the nuclei: at that point, the reaction rate was the highest.

In the case of *N*-oxide **I**, experimental data were fitted with the $f(\alpha) = 4(1-\alpha)^{3/4}$ function, pointing at chemical reaction as the rate-limiting stage [17]. Indeed, compound **I** was the only one occluding water; that pointed at low density of the crystal lattice and, hence, dehydration at stage 1 was accompanied with appearance of the lattice stresses and formation of the reactive sites.

To conclude, study of thermo-oxidative degradation of styryl derivatives of pyridine-*N*-oxides revealed their multi-stage character. Introduction of electron-donating substituents at position 4 of the pyridine ring enhanced thermo-oxidative stability of the compounds. 2-Styryl derivatives of the *N*-oxides were less thermally stable as compared with the 4-substituted isomers.

EXPERIMENTAL

The following compounds were studied: *N*-oxides of 4-styrylpyridine (**I**), 2-styrylpyridine (**II**), 4-(4'-chlorostyryl)pyridine (**III**), 4-(4'-dimethylaminostyryl)-pyridine (**IV**), 2-(4'-dimethylaminostyryl)pyridine (**V**), 4-(4'-methoxystyryl)pyridine (**VI**), and 2-(4'-me-

thoxystyryl)pyridine (**VII**). The listed compounds were prepared as described elsewhere [18–20].

Thermo-oxidative degradation of the listed *N*-oxides was studied using a thermoanalytical device including a 1000D derivatograph (MOM, Hungary) enabling simultaneous tracking of the sample temperature, the difference between the studied and the reference samples, the sample mass, and the rate of mass change [21]. Thermo-oxidative degradation of the *N*-oxides was performed in air at heating rate of 5 deg/min. The degradation onset was additionally monitored tracking the changes of electronic absorption spectra of aqueous solutions of the products (a UNICO 2800 spectrophotometer, USA).

Kinetic parameters of the studied processes were calculated via the Coats–Redfern method [22] based on combined analysis of kinetic equation $d\alpha/dt = kf(\alpha)$ (α, conversion degree; *t*, time; *k*, reaction rate constant) and the Arrhenius equation.

A 1 : 1 (w/w) mixture of $KMnO_4$ with Al_2O_3 was used as reference to ensure accurate determination of the kinetic parameters. The calculated activation energy of thermal degradation was of 140±1.0 kJ/mol with correlation coefficient of >0.995 coinciding with the reference data for the system [23].

REFERENCES

1. Lin, J.K. and Hurng, D.C., *Food Chem. Toxicol*., 1985, vol. 23, no. 6, p. 579.
2. Markowitz, J.S. and Patrick, K.S., *J. Chromatogr. (B),* 1995, vol. 668, no. 1, p. 171. DOI: 10.1016/0378-4347(95)00060-V.
3. Cashman, J.R., Park, S.B., Yang, Z.C., Wrighton, S.A., Jacob, III, P., and Benowitz, N.L., *Chem. Res. Toxicol*., 1992, vol. 5, no. 5, p. 639. DOI: 10.1021/tx00029a008.
4. Konkin, A., Wendler, F., Meister, F., Roth, H.K., Aganov, A., and Ambacher, O., *Spectrochim. Acta (A)*, 2008, vol. 69, no. 3, p. 1053. DOI: 10.1016/j.saa.2007.06.026.
5. Golova, L.K., Borodina, O.E., Belousov, Yu.Ya., Andreeva, I.N., Yablochko, L.P., and Papkov, S.P., *Fibre Chem*., 1987, vol. 19, no. 3, p. 204. DOI: 10.1007/BF00543852.
6. Saenz, L.R., Carreto-Vazquez, V.H., Rogers, W.J., Papadaki, M., and Mannan, M.S., *Catal. Commun*., 2011, vol. 12, no. 14, p. 1370. DOI: 10.1016/j.catcom.2011.03.036.
7. Soykan, C., Coskun, R., and Delibas, A., *Thermochim. Acta*, 2007, vol. 456, no. 12, p. 152. DOI: 10.1016/j.tca.2007.02.011.
8. Alker, D., Mageswaran, S., Ollis, W.D., and Hooshang Shahriari-Zavareh, *J. Chem. Soc., Perkin Trans. 1*, 1990, p. 1631. DOI: 10.1039/P19900001631.
9. Sammes, P.G., Serra-Errante, G., and Tinker, A.C., *J. Chem. Soc., Perkin Trans. 1*, 1979, p. 1736. DOI: 10.1039/P19790001736.
10. Jones, I.W., Kerr, D.A., and Wilson, D.A., *J. Chem. Soc. (C),* 1971, p. 2595. DOI: 10.1039/J39710002595.
11. Mackenzie, J., *Plant Oper. Prog*., 1991, vol. 10, no. 3, p. 164. DOI: 10.1002/prsb.720100310.
12. Papadaki, M., Marques-Domingo, E., Gao, J., and Mahmud, T., *J. Loss Prevent. Proc. Ind.,* 2005, vol. 18, nos. 4–6, p. 384. DOI: 10.1016/j.jlp.2005.06.024.
13. Gubarev, Yu.A., Lebedeva, N.Sh., V'yugin, A.I., Andreev, V.P., and Nizhnik, Ya.P., *Russ. J. Gen. Chem*., 2007, vol. 77, no. 6, p. 1093. DOI: 10.1134/S1070363207060254.
14. Suvorov, A.V., *Termodinamicheskaya khimiya paroobraznogo sostoyaniya* (Thermodynamic Chemistry of Vapor State), Leningrad: Khimiya, 1970.
15. *CRC Handbook of Chemistry and Physics*, Lide, D.R., Ed., Boca Raton: CRC Press; Taylor and Francis, 2009.
16. Palm, V.A., *Osnovy kolichestvennoi teorii organicheskikh reaktsii* (Fundamentals of the Quantitative Theory of Organic Reactions), Leningrad: Khimiya, 1967.
17. Samtani, M., Dollimore, D., and Alexander, K.S., *Thermochim. Acta*, 2002, vol. 392, p. 135. DOI: 10.1016/S0040-6031(02)00094-1.
18. Ochiai, E., *J. Org. Chem*., 1953, vol. 18, p. 534. DOI: 10.1021/jo01133a010.
19. *Svoistva organicheskikh soedinenii. Spravochnik* (Properties of Organic Compounds. Handbook), Potekhin, A.A., Ed., Leningrad: Khimiya, 1984.
20. Pentimalli, L., *Gazz. Chim. Ital*., 1963, vol. 93, p. 1093.
21. Lebedeva, N.Sh., Yakubov, S.P., Kinchin†, A.N., and V'yugin, A.I., *Russ. J. Phys. Chem. A.,* 2005, vol. 79, no. 5, p. 827.
22. Coats, A.W. and Redfern, J.P., *Nature*, 1964, vol. 201, p. 68.
23. Zatsepin, A.F. and Fotiev, A.A., *Zh. Neorg. Khim.*, 1973, vol. 18, no. 11, p. 2883.
24. Andreev, V.P., Sobolev, P.S., Zaitsev, D.O., and Il'yukhin, A.B., *Russ. J. Gen. Chem*., 2014, vol. 84, no. 1, p. 155. DOI: 10.1134/S1070363214010186.